Abbreviated Key Title: Glob. J. Environ. Sci. Technol.
ISSN: 2384-5058 (Print) & Open Access
Vol. 11(8): Pp 39-49, September, 2023.

Global Journal of Environmental Science and Technology: ISSN-2360-7955, (Print) & Open Access
Volume-11 | Issue-9| September, 2023 | Research Paper

Application of Numerical and Computational Based Models for Modelling the Effects of the Pore Size in Mild Steel TIG Welding Process

By

[1]Amadhe F. O, [1]Achebo J. I., [2]Obahiagbon K., *[1]Ozigagun A.

Corresponding author: Ozigagun A **Accepted: 20/8/2023 |** **Published: 9/9/2023**

[1]Department of Production Engineering, University of Benin, Benin City, Nigeria.
[2]Department of Chemical Engineering, University of Benin, Benin City, Nigeria.
E-mail: [1] francisoghenerurie@gmail.com, [1] joseph.achebo@uniben.edu, [2]kess.obahiagbon@uniben.edu,
Corresponding Author: *[1]andrewzigs@yahoo.com

Corresponding author: Ozigagun A . **Accepted: 20/8/2023 |** **Published: 9/9/2023**

Abstract: In order to lower production costs and create lightweight components, manufacturers are increasingly focusing on the combining of different materials. Welding with tungsten inert gas (TIG) is the chosen method for achieving a defect-free, reliable joint with a notably pleasing appearance. However, it's important to note that when dealing with materials that possess distinct chemical, physical, and thermal properties, special care is required to ensure the resulting joint is robust and rigid. This study delves into an investigation and modelling of TIG welding parameters concerning the size of pores and its impact on weld quality. The Response Surface Methodology (RSM) model has produced a numerical optimal solution consisting of a current of 200.72A, voltage of 20V, wire diameter of 2.40mm, and wire feed speed of 20m/s, which will yield a weld pore size of 0.195185. This solution was deemed optimal, boasting a desirability value of 93.9%, based on the design expert's evaluation. In parallel, an Artificial Neural Network (ANN) was employed in this study. For training purposes, 70% of the data was utilized, with 15% allocated for validation and the remaining 15% for the actual testing. The results have culminated in the creation of a regression plot, demonstrating the correlation between the input variables and the target variable, which yielded R2 values of 0.82928. Upon a comprehensive evaluation of the results, the Artificial Neural Network emerged as the superior predictive model compared to the Response Surface Methodology because the ANN output fits closer to the experimental than that of RSM. Thus, the approaches effectively optimized and predicted the weld pore size.

Keywords: *TIG welding, weld Pore size, RSM, ANN*

Published by GJEST

1. INTRODUCTION

When the right pressure, temperature, and metallurgical conditions are chosen during the welding process, two materials are permanently linked together through localized cohesion [1]. For combining copper-gold in the jewelry industry, welding has been used for a very long time [2]. Welding had already begun to develop quickly by the time electricity was widely available in the 19th century, and it was being used to combine metals. The terms "welding" and "brazing" are interchangeable when referring to the joining of autogenous metals [3]. Since the properties of the molten material related to fluid flow play a significant role in the process, the majority of researchers in the field explored the keyhole collapse events from a hydrodynamic point of view. Shifting the nozzle farther from the welding zone will, however, remove the fusion zone protection that shielding gases typically offer [4]. The authors suggested the ideal nozzle location, which is seen in Figures 1A–1C, where the gas widens the keyhole and makes it simpler for gases to escape from the welding pool during translation.

Figure 1A, 1B: Pore occurring after weld [5],

Figure 1C: Weld explode after TIG welding [6]

Using mechanical cleaning techniques such as scraping or employing a steel brush comes with a significant drawback: these methods inflict substantial damage to the parent material's surface, resulting in visible grooves and scratches. These surface imperfections have the potential to adversely affect the final appearance of the weld bead [7]. Furthermore, these techniques are challenging to control and heavily reliant on the operator's judgment for assessing cleanliness and ensuring repeatability. To overcome these limitations, numerical modelling has emerged as a highly effective tool for comprehending complex engineering issues [8]. Numerical simulations of engineering processes involve translating physical behaviors into mathematical relationships that can be analyzed and solved using computers, enabling the modelling of specific problems [9]. Modelling becomes particularly valuable when experimental or analytical approaches prove inadequate or in cases where laboratory work is prohibitively time-consuming, costly, or hazardous [10]. Welding different materials with varying chemical compositions, especially when using filler wires with distinct chemical compositions, complicates the observation of how filler wire composition influences porosity formation in welds [11]. In all arc welding processes, a method is employed to shield the molten weld pool from contact with the surrounding air. Submerged Arc Welding, in particular, is a favored approach due to its advantages, including high production rates, excellent melting efficiency, ease of automation, and a relatively low skill requirement for operators [12]-[14]. The quality of a weld is contingent on the bead geometry, which, in turn, hinges on various process variables.

2. METHODOLOGY

2.1 Experimental setup

A mobile phone camera was attached, placed above and to the side of the welding region, and programmed to take sequential pictures at a distance of 0.7m in order to record the spatter photos. Spatter shots taken in both the vertical and horizontal directions were combined to create two-dimensional spatter images. Spatter distribution is assessed using shots taken vertically, whereas spatter counting is carried out using photos taken horizontally. At 240 fps, scatter pictures were captured. Due to the welding arc's brilliance, the spatter photos that were collected were primarily distorted. As a result, welding spatter was only tracked using an optical filter. The digital lens was equipped with a neutral-density (ND) optical filter; an ND filter equally filters incident light across the wavelength spectrum, resulting in crisper images.

2.2 Design of experiment

A design of experiment is a scientific approach to organizing and carrying out an experiment that will reveal a cause-and-effect relationship between variables. It can also be a methodical approach to altering process inputs and analysing the resulting process outcomes so as to measure the cause-and-effect relationship between them as well as the random variability of the process while requiring the least amount of runs. Experimentation is a

crucial component of scientific research, which can be developed using computer softwares like design expert and Minitab. For appropriate polynomial approximation an experimental design is used to collect the data. There are different types of experimental designs which includes central composite circumscribed, central composite face centered, full factorial, and latin hyper cube designs.

.

2.3 Identification of range of input parameters

The primary considerations made in this study are welding voltage, welding current, wire diameter, and wire feed speed. Table 1 displays the variety of process parameters found in the literature

Table 1: Process parameters and their levels

Factors	Unit	Symbol	Low (-1)	High (+1)
Welding Current	Ampere	I	180	240
Welding Voltage	Volts	V	18	24
Wire diameter	Mn	WD	1.2	3.0
Wire feed speed	Mm/min	WFS	10	50

2.4 Materials and experimental set-up

For the experiments, 100 mild steel coupons with measurements of 80 x 40 x 10 (mm) were utilized. The investigation was conducted twenty times, with five samples per run. The plates' edges were machined and beveled before being welded using tungsten inert gas welding equipment. 10 mm thick plates of mild steel were TIG welded using different ranges of current, voltage, wire diameter and wire feed rate. In this research investigation, 100% pure Argon gas was employed as a shielding gas throughout the welding process to protect the weld specimen from air interaction. To prepare the welded samples, they were all cut perpendicular to the welding axis, mounted in resin, and then ground using silicon carbide abrasive sheets on a rotating disk in five stages of 80, 300, 600, 1200, and 4000 grits (Mecatech 334). After polishing with 3 µm (microns) and 1 µm diamond pastes, the specimens were then etched by immersing them in sodium hydroxide solution (1g NaOH + 100 ml H2O) as an etchant for 45 seconds. A digital microscope is utilized to model number KEYNCE VHX-500F, the samples' macrostructure and microstructure were investigated. Mild steel plate with a 10 mm thickness was used for the weld sample construction. The plate was powered hacksaw cut to size. Measurements and records of the reactions were made, the edges were ground, the surfaces were sanded with emery paper, and the connections were welded. The weld sample is shown in the figure below. In order to identify any phase changes at the cleaned surfaces, SEM was utilized to examine the laser-cleaned surfaces in comparison with a reference surface. The scanning electron microscope used was a Hitachi High Technologies S-3400N Type I, 0.1-30 kV microscope. Figures 2A and 2B depict the TIG apparatus, Figure 2C the spatter images, and Figure 2C the shielding gas cylinder and regulator.

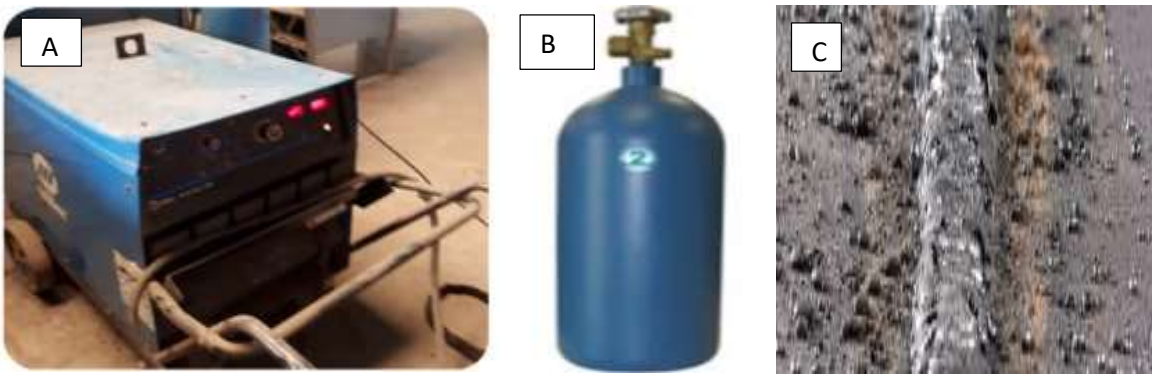

Figure 2: (A) TIG equipment **(B)** Shielding gas cylinder and regulator (**C)** Spatter images

2.5 Method of Data Collection

Using design expert software, the center composite design matrix was created, yielding 20 experimental runs. The experimental matrix is made up of the input and output parameters, as well as the outcomes noted for the data were taken from the weld sample. The data matrix is determined by the number of input parameters, which is provided by the equation 2n + 2n + k, where k is the quantity of center points, 2n is the quantity of axial points, and 2n is the quantity of factorial points. The data obtained were analysed using the Response Surface Methodology (RSM) and the Artificial Neural Network (ANN).

2.6 Response Surface Methodology

Response Surface Methodology (RSM) is a popular tool used by engineers to look for the circumstances that would best the desired procedure. In other words, they are looking for the process input parameter values that produce the best possible answers. The optimal value given as a function of the process's input parameters could be either a minimum or a maximum. To explain how the welding process performs as well as identify the response that is best, RSM is one of the optimization strategies that is currently in general use. RSM is a group of mathematical and statistical methods for prediction and modelling the interest response, which is influenced by a variety of input variables, with the aim of optimizing the response.

Table 2: Analysis of Variance Components

Variation Source	Degree of Freedom Df	Sum of Squares SS	Mean Square MS	Fisher Ratio F-value
Error of residuals	n-2	$SSE = \sum_{i=1}^{c}\sum_{j=1}^{ni}(y_{ij} - \hat{y}_{ij})^2$	$MSE = \frac{SSE}{n-2}$	
Regression	1	$SSR = \sum_{i=1}^{c}\sum_{j=1}^{ni}(\hat{y}_{ij} - \bar{y})^2$	$MSR = \frac{SSR}{1}$	$F = \frac{MSR}{MSE}$
Lack of fit	C -2	$SSLF_i = \sum_{i=1}^{c}\sum_{j=1}^{ni}(\bar{y}_{ij} - \hat{y}_{ij})^2$	$MSLF = \frac{SSLF}{c-2}$	$F^* = \frac{MSLF}{MSPE}$
Total	n-1	$SSTD = \sum_{i=1}^{c}\sum_{j=1}^{ni}(y_{ij} - \bar{y}_{ij})^2$	-	-

2.7 Artificial Neural Network

A neural network is a distributed, highly parallel computer that is naturally inclined to store experimental information and make it accessible for application. It is used as a data mining tool to identify unknown patterns in datasets. In two ways, it resembles the brain. A learning process occurs within the network, and synaptic weights—internal neuron connection strengths—are employed to store the knowledge. R input to an elementary neuron is weighted with the appropriate *w*. The input to the transfer function *f* is made up of the bias added to the weighted inputs. In order to generate their output, neurons can use any differentiable transfer function *f*. The transfer function logsig of a log-sigmoid is frequently applied to multilayer networks. The function logsig generates outputs between 0 and 1 as the neuron's net input changes from a negative value to a positive infinity. An alternative using the tan-sigmoid transfer function or tansig, in multilayer networks. Pattern recognition issues are frequently solved using sigmoid output neurons, whereas function fitting issues are typically solved using linear output neurons. The artificial neural network is a data mining tool, which uses the theory of the human brain and the neurone communication technique that has been programmed into a software. It is a predictive tool analyses a data by the following process: training, learning validating and testing.

3.0 RESULTS

In this study, two expert methods were used to examine the information gathered from the tests using the artificial

neural network (ANN) and the response surface methodology (RSM).

3.1 Modelling and Optimization using Response Surface Methodology (RSM)

The second order effects of non-linear relationships are included in the Response Surface Model, a modification on simple linear regression. Finding the ideal combinations of factors to determine a particular response to an event is a common optimization approach. RSM is particularly useful to understand the connection between multiple predictor variables with multiple predicted responses.

The optimization model's objective was to minimize the pore size. The optimization process's final answer was to establish the ideal value for each input variable, primarily current (Amp), voltage (V), wire diameter and wire feed speed that will give us the best weld output results.

To gather experimental data to aid in optimization.

i. A statistical design of experiment (DoE) was carried out utilizing the central composite design approach (CCD). The design and optimization were carried out with the assistance of a statistical tool. Design Expert 7.01 was used to solve this particular challenge.

ii. Thirty experimental runs were developed by an experimental design matrix containing six center points (k), eight axial points (2n), and sixteen factorial points (2n).

The sequential model sum of squares for pore size response was calculated to validate the quadratic model's applicability in evaluating the experimental data, as shown in Table 3.

Table 3: Sequential model sum of square for pore size

Source	Sum of Squares	df	Mean Square	F Value	p-value Prob > F	
Mean vs Total	4.10	1	4.10			
Linear vs Mean	0.085	4	0.021	1.30	0.2961	
2FI vs Linear	0.26	6	0.043	5.44	0.0020	
Quadratic vs 2FI	0.14	4	0.036	89.03	< 0.0001	Suggested
Cubic vs Quadratic	1.617E-003	8	2.021E-004	0.32	0.9341	Aliased
Residual	4.433E-003	7	6.333E-004			
Total	4.59	30	0.15			

The model statistics for the pore size response that were determined based on the model sources are displayed in Table 4.

Table 4: Model summary statistics for pore size

Source	Std. Dev.	R-Squared	Adjusted R-Squared	Predicted R-Squared	PRESS	
Linear	0.13	0.1725	0.0401	-0.2836	0.63	
2FI	0.089	0.6957	0.5355	0.4738	0.26	
Quadratic	0.020	0.9877	0.9762	0.9292	0.035	Suggested
Cubic	0.025	0.9910	0.9627	-0.2978	0.64	Aliased

The goodness of fit statistics reported in table 5 were used to assess the validity based on the quadratic model's capacity to minimize pore size.

Table 5: Goodness of fit statistics for pore size

Std. Dev.	0.020	R-Squared	0.9877
Mean	0.37	Adj R-Squared	0.9762
C.V. %	5.43	Pred R-Squared	0.9292
PRESS	0.035	Adeq Precision	39.551

To adopt any model, its suitability must first be validated by the results of an acceptable statistical investigation. To determine whether a value or group of values the model is unable to detect, the projected values are plotted against the actual values, as illustrated in Figure 5. The cook's distance plot was created for each

response to identify whether an outlier is likely present in the experimental data. The generated cook's distance for the pore size is presented in Figure 6.

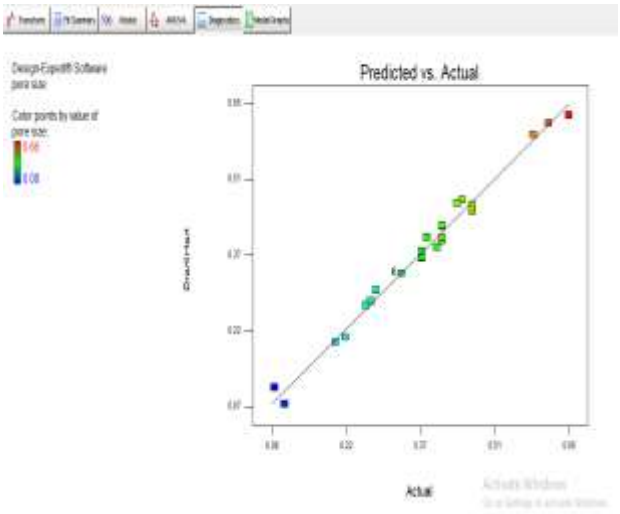

Figure 5: Plot of Predicted Vs Actual for pore size

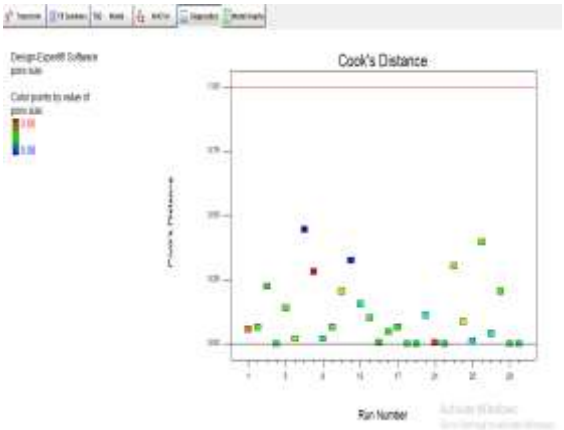

Figure 6: cook's distance plot for pore size

To investigate the impact of 3D surface plots of combined input factors on pore size are shown in Figure 7 was generated. To investigate the impact of 3D surface plots of combined input factors on pore size are shown in Figure 8.

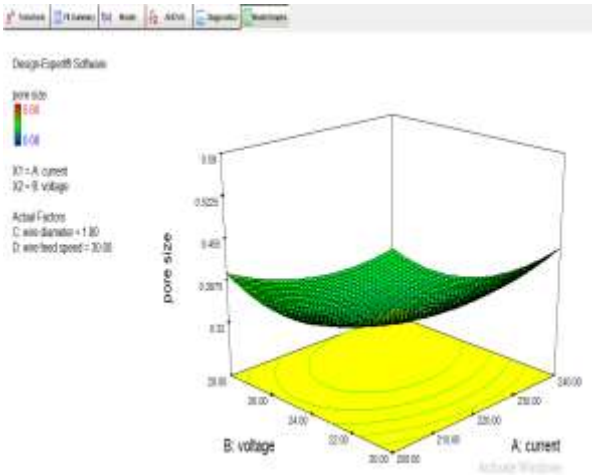

Figure 7: Effect of current and voltage on pore size

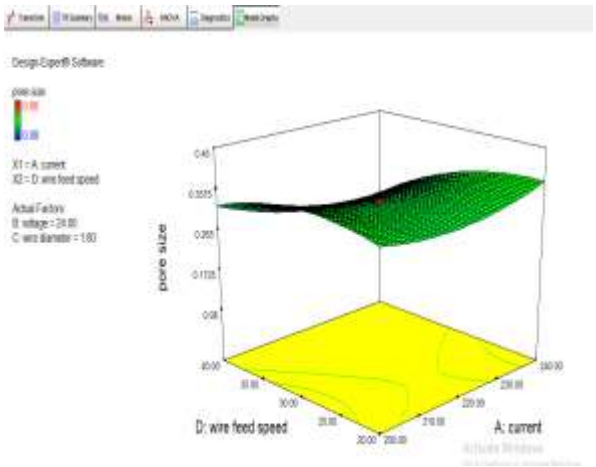

Figure 8: Effect of current and wire feed speed on pore size

3.2 Modelng and Optimization using Artificial Neural Network (ANN)

Inputs 'input' is a 4x30 matrix, 30 samples of four elements are used to represent static data. The 'pole size' of Targets is a 1x30 matrix that represents static data: 30 samples of 1 element. The ANN network architecture has 4 input , figure 9 depicts the network architecture pore size of 10 neurons in the hidden layer and 1 neuron in the output layer.

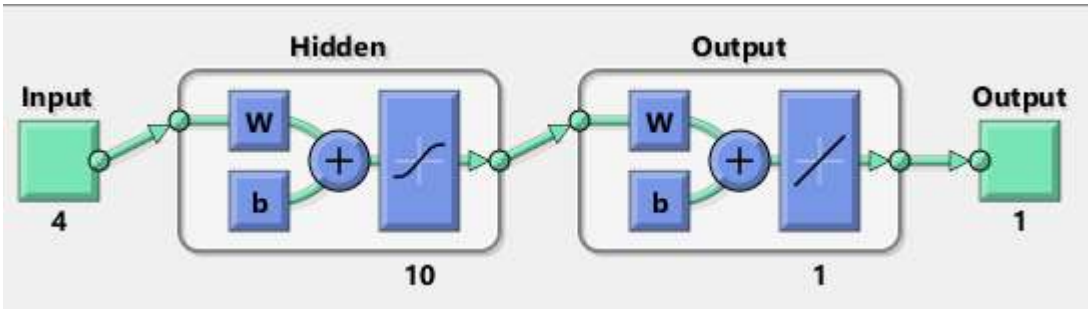

Figure 9: Artificial neural network architecture for predicting pore size

It is recommended that a set of data be set aside for validation and testing, therefore, that data obtained from this research were divided into three part with 70% of the experimental sample data, used for training 15% used for validation, while the remaining 15% was employed to put the neural network model to the test. It was noticed that the training of the network model provided a correlation having 85.4% with a mean square error of 15.47E-0. The validation of the network model produced a correlation of 89.6% with a mean square error of 12.84E-0. the testing of the network model produced a correlation of 73.8% with mean square error 46.56E-0.
.

The data division algorithm (dividerand), the training algorithm (trainlm), and the performance algorithm (mse) were all set to random. The pore size performance plot was created to test for network learning. At epoch 3, the best validation performance was obtained, which is shown in Figure 10. A gradient function plot is produced for the pore size network. It displays the number of epochs consumed throughout the training procedure. One epoch represents one entire algorithm training. Figure 11 demonstrates that the best prediction was attained at the third epoch, after using 5 epochs. The gradient function diagram is presented in figure 11

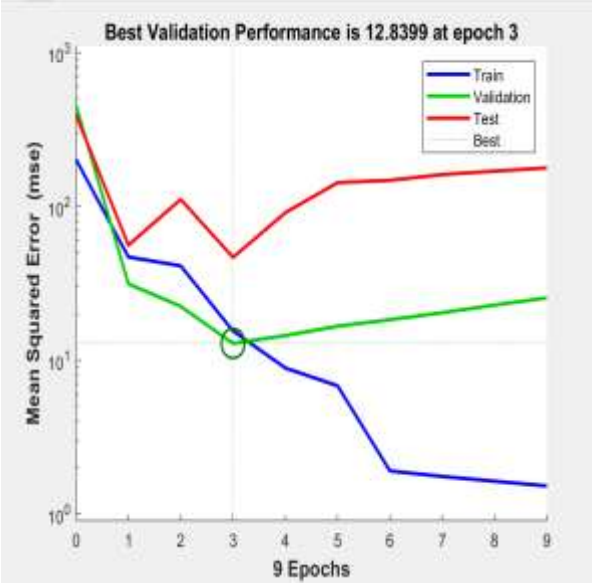

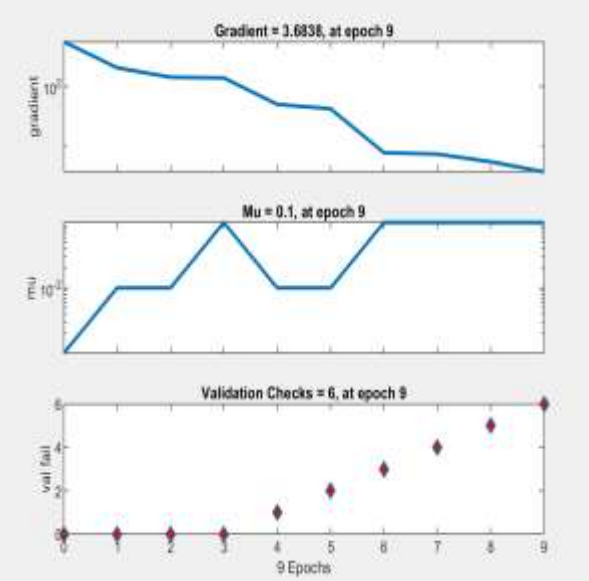

Figure 10: Performance curve for trained network to predicting Pore size responses Figure 11: Neural network gradient plot for predicting Pole size responses

A regression plot was produced to check the relationship that exists between the visible values and the network predicted values. The regression plot for the pore size network is presented in figure 12.

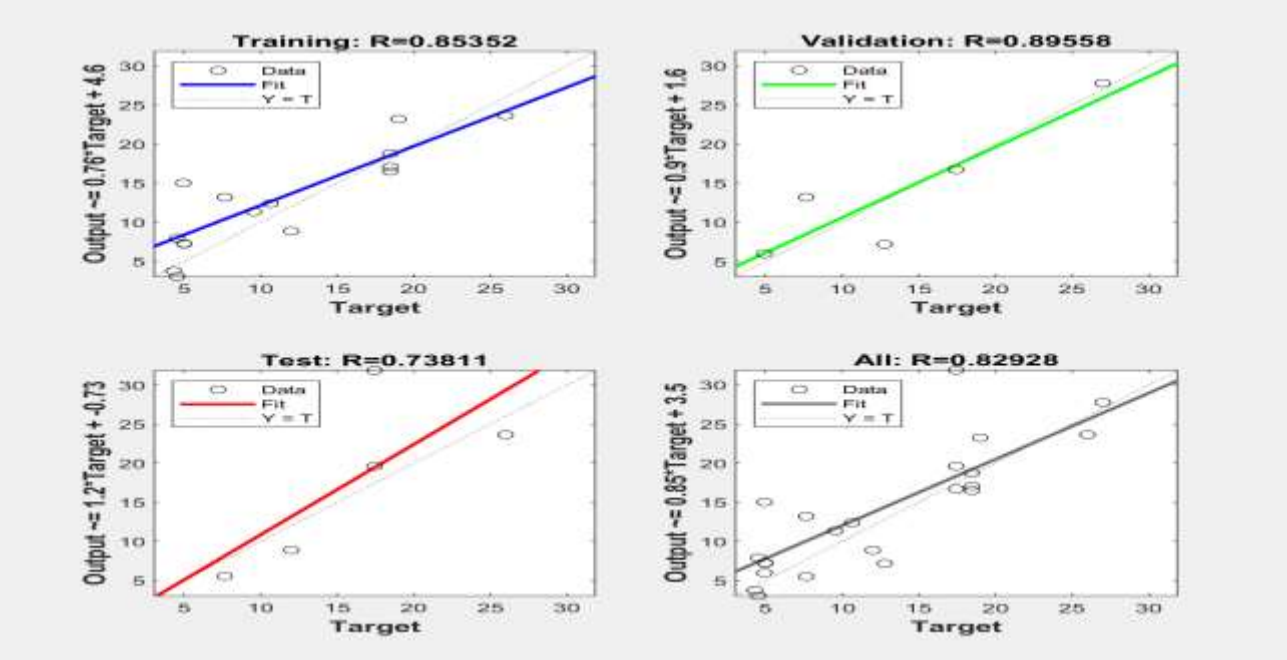

Figure 12: Regression plot of training, validation and testing for Pore size responses

Figure 12 shows a plot of training, validation, and testing with a correlation coefficient (R) of more than 70%, indicating a reliable prediction of pore size. The dotted diagonal line on each plot indicates the line of best fit which signals a perfect prediction and a correlation of 1
.

3.3 Comparison between the Experimental values, RSM and ANN values

A time series plot which can help to appreciate the graphical difference between the experimental result and the network output for pore size as shown in figure 13.

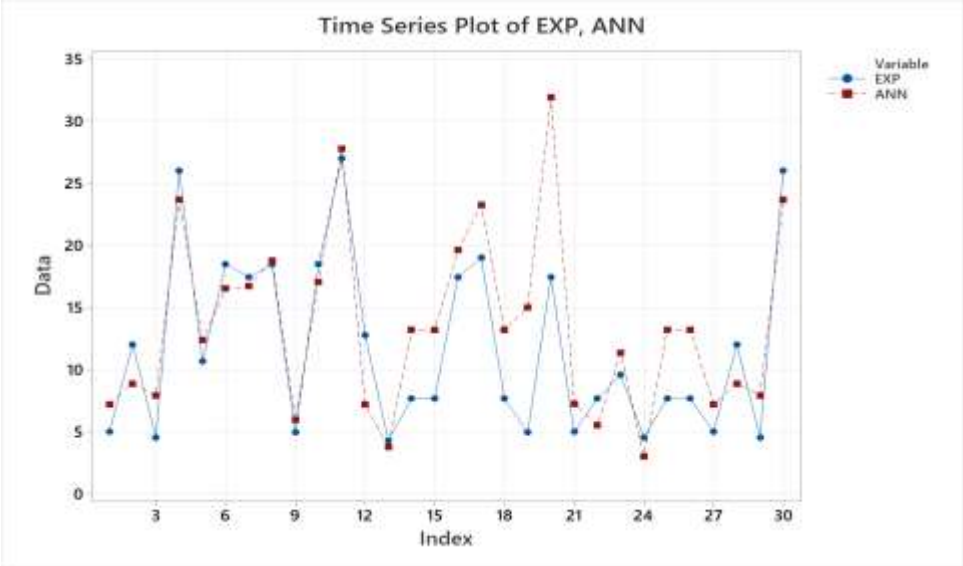

Figure 13: A time series plot for pore size

A fitted plot for the artificial network output was done to ilustrate the correlation between the experimental and the pore sizemodel developed,which is shown in figure 4.58

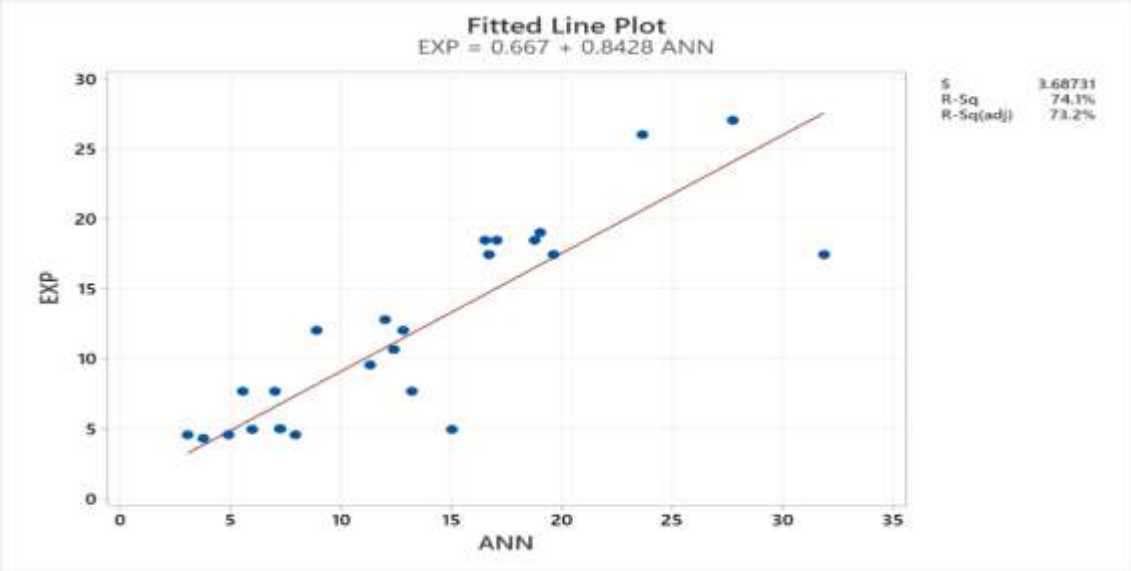

Figure 14: fitted line plot for the pore size

The regression equation is EXP = 0.667 + 0.8428 ANN

The model summary statistics for the pore size network is produced which shows the strength of the network output, the result is shown in table 6

.

Table 6: Model Summary

S	R-sq	R-sq(adj)
3.68731	74.12%	73.19%

The analysis of variance for the network output to check for the significance of the network as shown in table 7.

Table 7: Artificial Neural Network Analysis of Variance for pore size

Source	DF	SS	MS	F	P
Regression	1	1090.18	1090.18	80.18	0.000
Error	28	380.70	13.60		
Total	29	1470.87			

4.0 DISCUSSION

Two expert methods, namely, Response Surface methodology and the Artificial Neural Network have been used to explain the connection existing between welding process parameter and the pore size. The input parameters include current, voltage, wire diameter and wire feed speed. The first method used was the Response Surface methodology and the result obtained shows that the second order polynomial model best explains the behaviour of the experimental data. The link between process parameters and pore size is quadratic, with a substantial correlation between voltage, wire diameter and pore size with a p value < 0.00001. The variance

inflation factor (VIF) was 1.00 which shows that the model is substantial because a (VIF) greater than 10.00 is a cause for alarm. The goodness of fit statistics yielded a Coefficient of determination R^2 of 0.9877 to support the model's significance and appropriateness based on its ability to predict pore size. Finally, numerical optimization was obtained. With a desirability value of 0.939, Design Expert 7.01 software chose this solution as the best one. The second statistical tool used is the Artificial Neural Networks was also used to predict the electrode density, spatter index, pore size and porosity. The input data are divided into three sets at random. 70% of the resources are utilized to train the network, while 15% are used to assess network performance and 15% are used for the test. The levenberg marquardt algorithm was used for training. For the training interphase the network provided a correlation having 85.4% with a mean square error of 15.47E-0. The validation of the network model produced a correlation of 89.6% with a mean square error of 12.84E-0. the testing of the network model produced a correlation of 73.8% with mean square error 46.56E-0. The performance plot and the correlation plot showed that the network learnt accurately and can be used to predict the target responses.

5.0 CONCLUSION

The lesser the porosity in a weld structure, the better. Reducing weld defects and increasing weld quality improving reactions define weld quality and strength. The response surface methodology, and artificial neural network model were employed to predict and optimize these output parameters mentioned in this study. From the results obtained From the results, it is seen that (i) the ANOVA result showed that the lower the current and wire diameter the lower the porosity of the weld and (ii) the optimal solution of the RSM model is preferred as it is able to predict minimized porosity. Hence, the response surface methodology is selected as the best optimal solution. The application of expert systems, such as artificial neural network models and response surface techniques, increased the quality of tungsten inert gas welding. This research optimized welding response pore size, the optimal solution will help to produce welds with minimum pore size, thus, the strength, reliability and accuracy of the models have been tested and validated.

REFERENCES

[1] Dak, G.; Pandey, C. Experimental investigation on microstructure, mechanical properties, and residual stresses of dissimilar welded joint of martensitic P 92 and AISI 304 L austenitic stainless steel. *Int. J. Press. Vessel. Pip.* 2021, *194*, 104536.

[2] Khan, M.; Dewan, M.W.; Sarkar, M.Z. Effects of welding technique, filler metal and post-weld heat treatment on stainless steel and mild steel dissimilar welding joint. *J. Manuf. Processes* 2021, *64*, 1307–1321.

[3] Ramakrishnan, A.; Rameshkumar, T.; Rajamurugan, G.; Sundarraju, G.; Selvamuthukumaran, D. Experimental investigation on mechanical properties of TIG welded dissimilar AISI 304 and AISI 316 stainless steel using 308 filler rod. *Mater. Today Proc.* **2021**, *45*, 8207–8211.

[4] Satputaley, S.S.; Waware, Y.; Ksheersagar, K.; Jichkar, Y.; Khonde, K. Experimental investigation on effect of TIG welding process on chromoly 4130 and aluminum 7075-T6. *Mater. Today Proc.* 2021, *41*, 991–994.

[5] https://www.reddit.com/r/Welding/comments/347bgd/struggling_with_tig_on_stainless_steel/

[6] https://www.youtube.com/@weldHAGOJIBI/about

[7] Anbarasu, P.; Yokeswaran, R.; Godwin Antony, A.; Sivachandran, S. Investigation of filler material influence on hardness of TIG welded joints. *Mater. Today Proc.* 2020, *21*, 964–967.

[8] Kausar, A. Study of Weld Quality characteristics of Tungsten Inert Gas Welding of Dissimilar Metals SS 316L and IS 2062 Plates. *Int. J. Res. Appl. Sci. Eng. Technol.* 2019, *7*, 759–767.

[9] Hazari, H.R.; Balubai, M.; Suresh Kumar, D.; Haq, A.U. Experimental investigation of TIG welding on AA 6082 and AA 8011. In *Materials Today: Proceedings*; Elsevier: Amsterdam, The Netherlands, 2019; pp. 818–822.

[10] Sayed, A.R.; Kumbhare, Y.V.; Ingole, N.G.; Dhengale, P.T.; Dhanorkar, N.R. A Review Study of Dissimilar Metal Welds of Stainless Steel and Mild Steel by TIG Welding Process. *Int. J. Res. Appl. Sci. Eng. Technol.* 2019, *7*, 370–373.

[11] Kumar, A.; Sharma, V.; Baruaole, N.S. Experimental Investigation of TIG welding of Stainless Steel 202 and Stainless Steel 410 using Taguchi Technique. *Mody Univ. Int. J. Comput. Eng. Res.* 2017, *1*, 96–99.

[12] Maeda K, Suzuki R, Suga T, Kawahito Y (2020) Investigating delayed cracking behaviour in laser welds of high strength steel sheets using an X-ray transmission in-situ observation system. Sci Technol Weld Joi 25(5):377–382

[13] Ramadan, N.; Boghdadi, A. Parametric Optimization of TIG Welding Influence on Tensile Strength of Dissimilar Metals SS-304 and Low Carbon Steel by Using Taguchi Approach. *Am. J. Eng. Res.* 2020, *9*, 7–14.

[14] Vennimalai Rajan, A.; Mathalai Sundaram, D.C.; Vembathurajesh, A.; Nagaraja, R.; Chakravarthy Samy Durai, J.; Nagaraja, R. Analysis and Experimental investigation of Weld Characteristics for TIG Welding in Dissimilar Metals. *Int. J. Emerg. Trends Eng. Res.* 2020, *1*, 278–287.